Published in final edited form as:

Cancer Res. 2016 November 15; 76(22): 6543–6554. doi:10.1158/0008-5472.CAN-16-0438.

IGFBP2 activates the NF-κB pathway to drive epithelial-mesenchymal transition and invasive character in pancreatic ductal adenocarcinoma

Song Gao[1,2], **Yan Sun**[3], **Xuebin Zhang**[4], **Limei Hu**[1], **Yuexin Liu**[1], **Corrine Yingxuan Chua**[1], **Lynette M. Phillips**[1], **He Ren**[2], **Jason B. Fleming**[5], **Huamin Wang**[1], **Paul J. Chiao**[6], **Jihui Hao**[2], and **Wei Zhang**[1,6,7]

[1]Department of Pathology, The University of Texas MD Anderson Cancer Center, Houston, Texas, USA

[2]Department of Pancreatic Carcinoma, Tianjin Medical University Cancer Institute and Hospital, National Clinical Research Center for Cancer, Key Laboratory of Cancer Prevention and Therapy, Tianjin, PR China

[3]Department of Pathology, Tianjin Medical University Cancer Institute and Hospital, National Clinical Research Center for Cancer, Key Laboratory of Cancer Prevention and Therapy, Tianjin, PR China

[4]Department of Pathology, Tianjin Huanhu Hospital, Tianjin, PR China

[5]Department of Surgical Oncology, The University of Texas MD Anderson Cancer Center, Houston, Texas, USA

[6]Department of Molecular and Cellular Oncology, The University of Texas MD Anderson Cancer Center, Houston, Texas, USA

[7]Department of Cancer Biology, Comprehensive Cancer Center of Wake Forest Baptist Medical Center, Winston-Salem, NC, USA

Abstract

The molecular basis underlying the particularly aggressive nature of pancreatic ductal adenocarcinoma (PDAC) still remains unclear. Here we report evidence that the insulin-like growth factor-binding protein IGFBP2 acts as a potent oncogene to drive its extremely malignant character. We found that elevated IGFBP2 expression in primary tumors was associated with lymph node metastasis and shorter survival in PDAC patients. Enforced expression of IGFBP2 promoted invasion and metastasis of PDAC cells in vitro and in vivo by inducing NF-κB-dependent epithelial-mesenchymal transition (EMT). Mechanistic investigations revealed that IGFBP2 induced the nuclear translocation and phosphorylation of the p65 NF-κB subunit through

Corresponding authors: Wei Zhang, PhD, Department of Cancer Biology, Comprehensive Cancer Center of Wake Forest Baptist Medical Center, Winston-Salem, NC 27157, USA; Phone: 336-713-7508 wezhang@wakehealth.edu; or Jihui Hao, MD, PhD, Department of Pancreatic Carcinoma, Tianjin Medical University Cancer Institute and Hospital, National Clinical Research Center for Cancer, Key Laboratory of Cancer Prevention and Therapy, Tianjin PR China, 300060, Phone: 8622-2334-0123; haojihui@tjmuch.com.

Disclosures of Potential Conflicts of Interest: The authors have no conflicts of interest to disclose.

the PI3K/Akt/IKKβ pathway. Conversely, enforced expression of PTEN blunted this signaling pathway and restored an epithelial phenotype to PDAC cells in the presence of overexpressed IGFBP2. Overall, our results identify IGFBP2 as a pivotal regulator of an EMT axis in PDAC, the activation of which is sufficient to confer the characteristically aggressive clinical features of this disease.

Keywords

insulin-like growth factor–binding protein 2; epithelial-mesenchymal transition; pancreatic ductal adenocarcinoma; metastasis; p65

INTRODUCTION

Pancreatic ductal adenocarcinoma (PDAC) is estimated to have caused 39,590 deaths in the United States in 2014, ranking as the fourth leading cause of cancer death (1). Lack of an effective early diagnostic modality renders 80% of cases not amenable to radical tumor resection because of local and distant tumor spread (2). Even among patients who undergo surgery, the long-term prognosis remains dismal because of metastasis and recurrence (3). Thus, tracking and treatment of metastatic tumors remain the greatest challenges in the clinical management of PDAC.

Experimentally, metastasis can be closely modeled by augmented cellular migration and invasion, traits acquired by epithelial cells that are undergoing transition to the mesenchymal lineage. Epithelial-mesenchymal transition (EMT) was first identified as a developmental process that allows cells that are a part of a rigid architecture to escape and spread (4), which plays a central role in metastasis of PDAC (5, 6).

The insulin-like growth factor (IGF) system has recently been implicated in the progression of PDAC (7). IGF-binding protein 2 (IGFBP2) is one of six proteins in the IGFBP family that bind IGFs with high affinity (8). IGFBP2 expression has been shown to be elevated in many cancer types in both tumor cells (9–13) and in the plasma (14–16). Published studies showed that IGFBP2 was upregulated in pancreatic juice (17) and plasma (18) of PDAC patients. Whether IGFBP2 exhibits oncogenic activities in PDAC has not been elucidated. Of particular interest is the finding that IGFBP2 drives glioma progression through the integrin/integrin-linked kinase/NF-κB network (19), and NF-κB activation has been shown to be a key event in PDAC progression (20). As a vital inflammation–related transcription factor, NF-κB has been identified as a potent regulator of EMT (21–24).

In this study, we hypothesized that IGFBP2 is a key EMT inducer for PDAC and that this EMT induction is mediated through activation of the NF-κB–associated pathway. We tested the physiological relevance of this pathway in an *in vivo* model as well as in clinical samples.

MATERIALS AND METHODS

Human tissue specimens and immunohistochemical analysis

Through a protocol approved by the Ethics Committee of the Tianjin Cancer Institute and Hospital (Tianjin, China), tumor samples were obtained from 80 randomly selected PDAC patients treated at the hospital between 2000 and 2011. All 80 patients underwent radical pancreaticoduodenectomy with R0 margins confirmed by two pathologists. Station 1 and 2 lymph nodes around the pancreas (6, 8a, 8p, 12a, 12b, 12p, 13, 14p, 14d, and 17 group) were dissected routinely and assessed by two pathologists. No chemotherapy was administered before surgery. After the surgery, all the patients received standard chemotherapy (single-agent gemcitabine) for six cycles. No radiation therapy was given before or after surgery.

Consecutive sections of formalin-fixed, paraffin-embedded (FFPE) tumors were subjected to immunohistochemical (IHC) analysis for IGFBP2, PTEN, RELA (NF-κB subunit p65), E-cadherin, and vimentin (Table S1) using a DAB substrate kit (Maxin, Fuzhou, China) according to the manufacturer's instructions. The results were scored as described previously (25) by two pathologists blinded to the clinicopathologic data.

Cell culture and reagents

Human PDAC cell lines AsPc-1 and PANC-1 were purchased from ATCC (Rockville, MD). IKKβ$^{-/-}$ mouse embryonic fibroblasts (MEFs) were a kind gift from Dr. Michael Karin (University of California, Los Angeles, CA). IKKβ$^{-/-}$ MEFs and PANC-1 cells were cultured in Dulbecco modified essential medium (DMEM). AsPc-1 cells were cultured in RPMI-1640 medium. The media were supplemented with 10% fetal bovine serum (FBS). Cultures were incubated at 37°C in a humidified chamber with 5% CO_2. The PDAC cell lines were characterized or authenticated by ATCC using short tandem repeat profiling and passaged in our laboratory for fewer than 6 months before use.

The following reagents were used: protease and phosphatase inhibitor cocktails (Roche, Mannheim, Germany); PI3K inhibitor LY294002 and IKK inhibitor Bay117082 (Sigma-Aldrich, St. Louis, MO); and active full-length human IGFBP2 protein (Abcam, Cambridge, UK). Before treatment, the cells were starved overnight by incubation in serum-free medium. Patient-derived xenograft (PDX) cell lines MDA-PATC124, MDA-PATC102, MDA-PATC69, MDA-PATC53, MDA-PATC50, and MDA-PATC43 (Supplementary Fig. S1A) were established and cultured as previously reported (26).

SiRNA, plasmid construction, and transfection in PDAC cells

To induce stable expression of IGFBP2 in the cells, full-length human *IGFBP2* cDNA (Gene Bank no. NM_000597.2) was cloned into the pcDNA3.1 plasmid (Invitrogen, Grand Island, NY) and verified by sequencing. SiRNAs for targeted genes were designed by Sigma-Aldrich (siRNA-IGFBP2) and Cell Signaling Technology (Beverly, MA; siRNA-NF-κB-p65; Table S1).

For transfection, cells at 80% confluence were plated at a density of 5×10^5 cells/well in 6-well plates in medium containing 10% FBS. When the cells were 80% confluent, they were

transfected with 50 nM siRNAs or 4 μg plasmids in Lipofectamine 2000 (Invitrogen) for 48 hours. Stably transfected cells were selected by G418 treatment. The efficiency of IGFBP2 overexpression was evaluated by western blot. Mixed populations of IGFBP2-overexpressing cells were used for microarray analysis and orthotopic model construction. Clonal sublines were used for some cellular studies.

Western blot analysis

Whole-cell extracts were prepared by subjecting cells to lysis in RIPA buffer supplemented with a proteinase inhibitor cocktail. The nuclear and cytoplasmic components were fractionated by using the NE-PER Nuclear and Cytoplasmic Extraction Reagents kit (Thermo Fisher Scientific, Waltham, MA) according to the manufacturer's protocol. Protein lysates (20 μg) were separated by sodium dodecyl sulfate polyacrylamide gel electrophoresis, and target proteins were detected by western blot.

Animal experiments and measurement of metastasis in an orthotopic model

Female 4-week-old nude nu/nu mice were maintained in a barrier facility on high-efficiency particulate air-filtered racks. All animal studies were conducted under a protocol approved by IACUC in accordance with the principles and procedures outlined in the NIH Guide for the Care and Use of Laboratory Animals. Thirty mice were divided into two groups (15 mice/group): one group was injected with mixed populations from IGFBP2-overexpressing AsPc-1 cells and the other group with AsPc-1 cells transfected with empty vector (EV). As previously described (27), cells were harvested by trypsinization, washed in phosphate-buffered saline solution (PBS), and resuspended at 10^7 cells/mL in a 1:1 solution of PBS/Matrigel. For each mouse, the pancreas was exposed and injected with 50 μL of cells in suspension. Six weeks later, all of the mice were sacrificed and necropsied for observation of visible metastatic lesions in the mesentery. The primary and metastatic pancreatic tumors were excised, weighed, fixed in formalin, and embedded in paraffin. Half of the tissues were subjected to hematoxylin and eosin and IHC staining as described for human PDAC tumors. The other half was subjected to western blot.

Gene expression profiling and pathway analyses

Microarray analysis for the mixed population of IGFBP2-overexpressing AsPc-1 cells was carried out by using the Human Whole Genome Oligo Microarray Kit from Agilent Technologies (Santa Clara, CA) as described previously (19). Expressed RELA (p65)-targeted genes were overlaid onto a global molecular network developed from information contained in the Ingenuity Pathways Knowledge Base (IPA Ingenuity Systems; Qiagen, Redwood City, CA). The network of these RELA-targeted genes was then algorithmically generated on the basis of their connectivity, and the molecular relationships between these genes/gene products were presented graphically. Microarray data have been deposited to GEO (accession number GSE64611).

Wound healing and invasion assays

The wound-healing assay was performed according to a published protocol (28). Invasion assays were performed in Matrigel-coated transwell invasion chambers with an 8.0-μm pore

size (BD Biosciences, San Jose, CA). For this assay, 1×10^5 cells were added into the upper chamber containing 500 μL of serum-free DMEM. Another 750 μL of DMEM with 10% FBS was added into the lower chamber, and the cells were allowed to invade for 24 hours. The cells that invaded through the filter into the lower chamber were stained with a three-step process (Thermo Scientific) and counted. Each experiment was performed in triplicate, and mean values are presented.

Immunofluorescence imaging

Cell suspensions (30 μL at a density of 1×10^6 cells/mL) were placed in a μ-Slide VI cell microscopy chamber (Ibidi Integrated BioDiagnostics, Munich, Germany) and allowed to adhere for 30 minutes. The immunostaining and imaging were carried out as described previously (28).

Luciferase reporter assay

AsPc-1 cells were co-transfected with pGL4.32 (luc2NF-κB-RE/Hygro) vector and pRL4-TK *Renilla* luciferase constructs (Promega, Fitchburg, WI) via Lipofectamine 2000 (Invitrogen) as previously described (29). Twenty-four hours later, the cells were transfected with pcDNA3.1-IGFBP2 plasmids, with or without pretreatment with Ly294002 (50 μM) or Bay117082 (20 μM). A dual luciferase reporter assay (Promega) was performed 24 hours after transfection and treatment according to the manufacturer's instructions, and luciferase activity was measured with a TD-20/20 luminometer. Each assay was performed in triplicate, and all firefly luciferase values were normalized to *Renilla* luciferase readings.

Statistical analysis

The Student *t*-test for paired data was used to compare mean values. ANOVA was used to compare continuous variables between groups. Non-parametric data were analyzed with the Mann-Whitney U test. The categorical data were analyzed by either the Fisher exact or the chi-square method. The log-rank test was used to obtain a *P*-value for the significance of divergence of Kaplan–Meier curves. All probability values were two-sided. Analyses were performed with the SPSS version 22.0 and Graphpad Prism 6.02 statistical analysis software.

RESULTS

Overexpressed IGFBP2 is a driver of lymph node metastasis and is correlated with shorter survival in PDAC

IHC staining showed that IGFBP2 was expressed in tumor cells but rarely in adjacent normal pancreatic cells (Fig. 1A). Western blot showed that IGFBP2 expression was significantly higher in tumor tissue than adjacent tissue in seven of the eight pairs tested (Fig. 1B, $P<0.001$). Moreover, IGFBP2 level (Supplementary Fig. S1B) was significantly correlated with lymph node metastasis ($P<0.001$; Fig. 1C, Supplementary Fig. S1C; Table S2). Notably, patients whose tumor expressed a high level (++/+++) of IGFBP2 had significantly shorter overall survival than those whose tumor expressed no or a low level (−/+) of IGFBP2 (median survival time: 13 months versus 20 months, $P=0.0018$; Fig. 1D).

To determine whether IGFBP2 promotes PDAC cell metastasis, we constructed an orthotopic PDAC mouse model with IGFBP2-overexpressing and vector-transfected control AsPc-1 cells (Supplementary Fig. S1D). The expression of IGFBP2 in both primary and metastatic lesions was higher in the IGFBP2-overexpressing group than in the control group (Supplementary Fig. S1E). Compared with the control group, the mice with IGFBP2-overexpressing tumors had more mesenteric lymph node metastasis (Fig. 1E–F). However, the orthotopic tumors from the two groups did not differ in size or weight (Supplementary Fig. S1F–G), which indicates that IGFBP2 facilitated invasion rather than proliferation of PDAC cells. These findings together strongly indicate that IGFBP2 plays a critical role in PDAC progression and is related to patient prognosis.

IGFBP2 promotes EMT in PDAC cells

The clinical and *in vivo* findings of an association between IGFBP2 and lymph node metastasis prompted us to examine the molecular events modulated by IGFBP2 in PDAC cells. Microarray analysis of the mixed population of IGFBP2-expressing AsPc-1 cells and control cells generated a heatmap representing 1,912 genes differentially expressed between the two groups (>1.5-fold change cut-off value; Fig. 2A). We noted that mesenchymal markers vimentin and Snai1 were upregulated at the transcriptional level in the IGFBP2-expressing cells, while epithelial marker CDH1 (E-cadherin) was significantly downregulated. During the selection of stable clones, observable changes were already evident; IGFBP2-expressing cells exhibited elongated and spindle-like morphologies indicative of EMT (Supplementary Fig. S2A).

In both AsPc-1 cells and PDX cell lines MDA-PATC50 and MDA-PATC124, western blot showed that IGFBP2 overexpression led to reduction of E-cadherin expression and increase of N-cadherin, vimentin, and Snai1 expression (Fig. 2B, Supplementary Fig. S3A–B). Immunofluorescence revealed decreased E-cadherin expression in cell-cell junctions in IGFBP2-expressing mesenchyme-like MDA-PATC50 cells (Fig. 2C) as well as stable IGFBP2-expressing AsPc-1 clones (Supplementary Fig. S2B). Wound-healing and Boyden chamber transwell assays showed that elevated IGFBP2 expression led to significant increases in cell migration and invasion (Supplementary Fig. S2D–F).

In contrast, the opposite effects were observed in MDA-PATC69, MDA-PATC102, and PANC-1 cells in which IGFBP2 was knocked down: E-cadherin expression was higher in knockdown cells, and expression of Snai1, N-cadherin, and vimentin was lower (Fig. 2D, Supplementary Fig. S3C–D). Immunofluorescence also manifested an epithelial phenotype in the knockdown cells, characterized by a typical cobblestone staining pattern with strong E-cadherin staining highlighting the cell-cell junctions compared to control cells (Fig. 2E, Supplementary Fig. S2C). Migration and invasion capacities of the knockdown cells were attenuated (Supplementary Fig. S2G–I).

IGFBP2 promotes EMT through NF-κB signaling

To investigate the signaling pathway involved in IGFBP2-induced EMT, we analyzed microarray data with Ingenuity Pathway Analysis (IPA), which revealed that RELA (p65) was the most affected transcriptional factor in the upstream regulator rankings based on its

P-value ($P=1.83\times10^{-9}$) with overlapping dataset genes (Fig. 3A). Genes downstream from NF-κB displayed a well-interconnected regulatory system with RELA as a central node (Fig. 3B). The expression direction (increase or decrease) of these RELA-targeted genes is consistent with activation of the NF-κB pathway.

Activation of NF-κB is known to require translocation of the p65 subunit from the cytoplasm to the nucleus. To validate the results of the microarray analysis, we examined the nuclear localization of p65 protein by western blot of fractionated proteins or by immunofluorescence in PDX cell lines. Levels of the activated nuclear form p-p65 were significantly higher in IGFBP2-expressing MDA-PATC50 and MDA-PATC124 PDX cells than in EV-transfected cells (Fig. 3C–D, Supplementary Fig. S3E). AsPc-1 cells showed similar p65 transnuclear localization following IGFBP2 overexpression, accompanied by decreased E-cadherin and increased vimentin expression (Fig. 4A–B, Supplementary Fig. S3G). Knockdown of IGFBP2 in MDA-PATC102 and MDA-PATC69 PDX cell lines, on the other hand, led to decreased expression of nuclear p-p65 protein (Fig. 3E–F, Supplementary Fig. S3F). Knockdown of IGFBP2 in PANC-1 cells also attenuated p65 transnuclear localization, increased expression of E-cadherin, and decreased expression of vimentin relative to levels in control cells (Fig. 4C–D, Supplementary Fig. S3H).

To determine whether activation of NF-κB is required for IGFBP2-induced EMT, p65 was suppressed in IGFBP2-overexpressing AsPc-1 cells by siRNA (Supplementary Fig. S4A). The knockdown of p65 blocked the IGFBP2-induced changes in expression of E-cadherin and vimentin (Fig. 4E, Supplementary Fig. S3I) and the associated EMT phenotype (Fig. 4F), as well as in cell migration and invasion (Fig. 4G–I). Thus, IGFBP2 failed to promote EMT and cell migration and invasion when NF-κB was blocked, indicating that IGFBP2 induction of EMT is dependent on NF-κB.

IGFBP2 activates NF-κB through the PI3K/Akt/IKKβ pathway by inhibiting PTEN during EMT

NF-κB activation in RAS-transformed cells is known to be mediated through the PI3K/Akt pathway (30). Moreover, our previous study found that IGFBP2 is involved in activation of the Akt pathway in glioblastoma (31). Thus we hypothesized that IGFBP2 activates NF-κB through the PI3K/Akt pathway in PDAC. To test this, we first treated AsPc-1 cells with recombinant IGFBP2 protein (Supplementary Fig. S4B) and found that p-Akt, nuclear p65, and p-p65 were all upregulated in a time-dependent manner (Supplementary Fig. S4C).

A key kinase for NF-κB activation is IκB kinase beta (IKKβ), which releases subunit p65 from IκBα and facilitates its nuclear translocation (32, 33). Because our data show that IGFBP2 activated Akt and promoted nuclear translocation of p65, we investigated whether IKKβ is involved in activation of NF-κB by IGFBP2 through PI3K/Akt. Co-immunoprecipitation demonstrated the interaction of Akt and IKKβ to form a complex (Supplementary Fig. S4E). Further analysis showed that IGFBP2 activated Akt in both IKKβ–wild-type and -null MEFs; however, NF-κB was activated only in wild-type MEFs, not in IKKβ-null MEFs (Fig. 5A, Supplementary Fig. S5A). These results suggest that IKKβ is required for IGFBP2 activation and translocation of NF-κB.

To further validate the involvement of PI3K/Akt and IKKβ in NF-κB activation, we adopted a pharmacologic approach. After pretreatment with PI3K inhibitor LY294002 (50 μM) or IKK inhibitor Bay117082 (20 μM) for 1 or 4 hours, AsPc-1 cells were treated with IGFBP2 (100 ng/mL). A dose-response analysis was performed as a preliminary experiment to rule out off-target effects (Supplementary Fig. S4F). The results show that IGFBP2 failed to activate p65 when either the PI3K/Akt or the IKK pathway was blocked (Fig. 5B, Supplementary Fig. S4G, Supplementary Fig. S5B). Furthermore, luciferase reporter assays demonstrated that NF-κB transcriptional activity was significantly greater in transiently IGFBP2-transfected AsPc-1 than in EV-transfected cells ($P<0.001$; Fig. 5C). NF-κB transcriptional activity was decreased by treatment with either the PI3K or IKK inhibitor ($P<0.05$; Fig. 5C).

To further investigate the effects of IGFBP2 on NF-κB activation, we knocked down endogenous IGFBP2 in PANC-1 cells. Knocking down IGFBP2 led to decreases of both Akt and IKKβ phosphorylation as well as p65 and p-p65 nuclear translocation, which were restored by treatment with exogenous IGFBP2 (Fig. 5D, Supplementary Fig. S5C). In stable IGFBP2-overexpressing cells, treatment with these inhibitors not only showed the same effect on IGFBP2 activation of the PI3K/Akt/IKKβ/p65 pathway but also restored the expression of E-cadherin, indicating that blockage of the PI3K/Akt/IKKβ/p65 pathway reversed IGFBP2-induced EMT (Fig. 5E, Supplementary Fig. S5D).

To clarify whether activation of the PI3K/Akt pathway by IGFBP2 is mediated through IGF1R, we treated AsPc-1 cells with recombinant IGFBP2 protein. IGFBP2 failed to induce phosphorylation of IGF1R (Supplementary Fig. S4D). We then investigated the role of PTEN, a key upstream suppressor for PI3K/AKT signaling that has been widely assumed to be a minimally relevant tumor suppressor in PDAC (32), in the IGFBP2-activated PI3K/Akt pathway. We first evaluated the association between IGFBP2 and PTEN expression in consecutive sections of FFPE samples from the patient cohort and found an inverse association between them (Fig. 6A–B). A similar pattern of expression of the two proteins was observed in PDX cell lines (Fig. 6C). We next transfected IGFBP2 plasmid into MDA-PATC50 and AsPc-1 cells or IGFBP2 siRNA into MDA-PATC69 and PANC-1 cells. Western blots showed an inverse effect of IGFBP2 expression on PTEN levels in transfected cells (Fig. 6D, Supplementary Fig. S6A). However, PTEN transcript levels did not change after modulation of IGFBP2 expression (Supplementary Fig. S6B), which indicates that the regulation was at a post-transcriptional level.

To further examine the role of PTEN in IGFBP2-induced EMT, we transfected stable IGFBP2-overexpressing AsPc-1 cells with either wild-type PTEN or a mutant PTEN (G129E) in which the ability to recognize inositol phospholipids as a substrate was lost. Expression of wild-type PTEN inhibited the nuclear translocation of p65 and restored E-cadherin expression and epithelial phenotype in these cells, whereas the mutant PTEN failed to induce these effects (Fig. 6E–F, Supplementary Fig. S6C).

In vivo validation of IGFBP-2/p65/EMT axis activation and its clinical importance in PDAC

To ascertain that our cell-based mechanistic findings are relevant in *in vivo* models, we performed IHC staining in consecutive tumor sections from the mouse models. We observed

an inverse expression pattern of PTEN (P=0.0349) and E-cadherin (P=0.0287) as well as a positive correlation of nuclear p65 (P=0.01) in the IGFBP2-expressing tumors (Fig. 7A–B). Similar patterns of IGFBP2, p65, E-cadherin, and vimentin expression were observed in consecutive sections of tumor samples from the patient cohort (Fig. 7C). As shown in Figure 7D, IGFBP2 expression was positively correlated with nuclear p65 (P<0.001) and vimentin (P<0.001) expression and inversely correlated with E-cadherin expression (P<0.001). These data suggest the existence of an IGFBP2/p65/EMT axis in PDAC tumors. Furthermore, the expression levels of nuclear p65, E-cadherin, and vimentin were strongly correlated with lymph node metastasis individually (Table S3). The Kaplan-Meier overall survival curves showed that high nuclear p65 expression, low E-cadherin expression, and high vimentin expression were associated with shorter survival (Fig. 7E), further supporting the clinical significance of this novel pathway. Examination of the expression of four other well-known members of the IGFBP family in PDAC tumors from the patient cohort (Supplementary Fig. S7A–B) found that IGFBP2 was the only member whose expression showed clinically relevant differences (Supplementary Fig. S7C). Taken together, the IHC staining and clinical data strengthen our conclusion that IGFBP2 promotes EMT in an NF-κB–dependent manner, which may contribute to lymph node metastasis and thus to poor outcome for PDAC patients.

DISCUSSION

The present study provides clinical and experimental evidence to support the oncogenic role of IGFBP2 in PDAC. Our results also highlight the clinical significance of IGFBP2 in PDAC. We found that patients whose tumor exhibited a high level of IGFBP2 had higher risk of peri-pancreas lymph node metastasis, which is an independent prognostic factor in PDAC (34). These findings improve our understanding of IGFBP2 biology and may help clinicians predict the risk of lymph node metastasis for patients whose primary tumor expresses a high level of IGFBP2.

There is increasing evidence that EMT represents the key cellular reprogramming required for metastasis and chemoresistance in PDAC (35). Several growth factors have been documented to trigger EMT (36). While TGFB1 often overexpressed in PDAC, is the most well-known EMT inducer, it also exhibits tumor suppressor functions (37). Thus, it is unclear whether TGF-β is a valid therapeutic target for PDAC (38). In this study, we identified IGFBP2 as a novel EMT inducer in cell lines that are known as either responsive (PANC-1) or unresponsive (AsPc-1) to TGF-β (39). In AsPc-1 cells, IGFBP2 overexpression resulted in EMT, whereas in PANC-1 cells, IGFBP2 knockdown led to the reverse, mesenchymal-epithelial transition. These results show that IGFBP2 induction of EMT in PDAC cells was likely independent of TGF-β.

Our mechanistic studies show that IGFBP2's induction of EMT was mediated through activation of NF-κB, a recognized event in PDAC (40). NF-κB has been shown to be essential for the EMT process (22). Our microarray data reveal several EMT-related genes in the IGFBP2-activated NF-κB network. *Snai1* has been shown to be stabilized by NF-κB through blockage of ubiquitination (41). The well-known mesenchymal marker vimentin was proven to be a driver for EMT in our recent study (42). Although vimentin is not

included in the RELA network produced by our IPA analysis, it has been shown to have a binding site for NF-κB on its promoter and is regarded as directly regulated by NF-κB (43).

Although PTEN missense mutations rarely occur in human PDAC (44), there is evidence supporting alternative mechanisms for loss of PTEN function and PTEN-controlled pathways (45), such as increased p-Akt (46). The literature suggests an inverse relationship between IGFBP2 and PTEN in glioblastoma and prostate cancer cells (47). Recent reports showed that, in vascular smooth muscle (48) and osteoblast cells (49), IGFBP2 inactivated PTEN by suppressing the receptor protein tyrosine phosphatase β (RPTPβ), which stabilizes PTEN. Our data consistently show an inverse regulatory and functional relationship between IGFBP2 and PTEN in PDAC. Through counteracting IGFBP2 function, PTEN overexpression repressed NF-κB activation and inhibited EMT.

In summary, our study of IGFBP2 expression in a cohort of PDAC patients and in *in vitro* PDX and tumor cell lines provides evidence that expression of IGFBP2 in PDAC contributes to its progression, thus implicating IGFBP2 as a potential therapeutic target as well as a valuable biomarker for evaluating prognosis and determining appropriate surgical strategy for PDAC patients.

Supplementary Material

Refer to Web version on PubMed Central for supplementary material.

Acknowledgments

Financial Support: This study was partially supported by a grant from the U.S. National Institutes of Health (U24CA143835) and the MD Anderson Cancer Center support grant (P30CA016672), a grant from the National Foundation for Cancer Research (to W. Zhang), grants (81302082, 81172355) from the National Natural Science Foundation of China (to J.H. Hao), and a grant (31301151) from the National Natural Science Foundation of China (to S. Gao). W. Zhang is supported by the Hanes and Willies Family Professorship in Cancer at Wake Forest Baptist Medical Center.

We thank Dr. Anirban Maitra (Department of Pathology, MD Anderson Cancer Center) for valuable discussion and input, Dr. Michael Karin (University of California, Los Angeles, CA) for providing the IKK-null MEFs, Dr. Jared Burks (Flow Cytometry & Cellular Imaging Core Facility, MD Anderson Cancer Center) for technical assistance, and Ms. Kathryn Hale (Department of Scientific Publications, MD Anderson Cancer Center) for editing the manuscript.

References

1. American Cancer Society. Cancer facts & figures 2014. Atlanta, GA: American Cancer Society; 2016 Aug 22. http://www.cancer.org/research/cancerfactsstatistics/cancerfactsfigures2014
2. Stathis A, Moore MJ. Advanced pancreatic carcinoma: current treatment and future challenges. Nat Re Clin Oncol. 2010; 7:163–72.
3. Benckert C, Thelen A, Cramer T, Weichert W, Gaebelein G, Gessner R, et al. Impact of microvessel density on lymph node metastasis and survival after curative resection of pancreatic cancer. Surg Today. 2012; 42:169–76. [PubMed: 22068680]
4. Thiery JP, Acloque H, Huang RY, Nieto MA. Epithelial-mesenchymal transitions in development and disease. Cell. 2009; 139:871–90. [PubMed: 19945376]
5. Rhim AD, Mirek ET, Aiello NM, Maitra A, Bailey JM, McAllister F, et al. EMT and dissemination precede pancreatic tumor formation. Cell. 2012; 148:349–61. [PubMed: 22265420]

6. Rasheed ZA, Yang J, Wang Q, Kowalski J, Freed I, Murter C, et al. Prognostic significance of tumorigenic cells with mesenchymal features in pancreatic adenocarcinoma. J Natl Cancer Inst. 2010; 102:340–51. [PubMed: 20164446]

7. Subramani R, Lopez-Valdez R, Arumugam A, Nandy S, Boopalan T, Lakshmanaswamy R. Targeting insulin-like growth factor 1 receptor inhibits pancreatic cancer growth and metastasis. PloS One. 2014; 9:e97016. [PubMed: 24809702]

8. Yu H, Rohan T. Role of the insulin-like growth factor family in cancer development and progression. J Natl Cancer Inst. 2000; 92:1472–89. [PubMed: 10995803]

9. Lee EJ, Mircean C, Shmulevich I, Wang H, Liu J, Niemisto A, et al. Insulin-like growth factor binding protein 2 promotes ovarian cancer cell invasion. Mol Cancer. 2005; 4:7. [PubMed: 15686601]

10. Moore LM, Holmes KM, Smith SM, Wu Y, Tchougounova E, Uhrbom L, et al. IGFBP2 is a candidate biomarker for Ink4a-Arf status and a therapeutic target for high-grade gliomas. Proc Natl Acad of Sci U S A. 2009; 106:16675–9. [PubMed: 19805356]

11. Wang H, Wang H, Shen W, Huang H, Hu L, Ramdas L, et al. Insulin-like growth factor binding protein 2 enhances glioblastoma invasion by activating invasion-enhancing genes. Cancer Res. 2003; 63:4315–21. [PubMed: 12907597]

12. Fuller GN, Rhee CH, Hess KR, Caskey LS, Wang R, Bruner JM, et al. Reactivation of insulin-like growth factor binding protein 2 expression in glioblastoma multiforme: a revelation by parallel gene expression profiling. Cancer Res. 1999; 59:4228–32. [PubMed: 10485462]

13. Chua CY, Liu Y, Granberg KJ, Hu L, Haapasalo H, Annala MJ, et al. IGFBP2 potentiates nuclear EGFR-STAT3 signaling. Oncogene. 2016; 35:738–747. [PubMed: 25893308]

14. Huynh H, Zheng J, Umikawa M, Zhang C, Silvany R, Iizuka S, et al. IGF binding protein 2 supports the survival and cycling of hematopoietic stem cells. Blood. 2011; 118:3236–43. [PubMed: 21821709]

15. Lin Y, Jiang T, Zhou K, Xu L, Chen B, Li G, et al. Plasma IGFBP-2 levels predict clinical outcomes of patients with high-grade gliomas. Neuro-oncology. 2009; 11:468–76. [PubMed: 19164435]

16. Liou JM, Shun CT, Liang JT, Chiu HM, Chen MJ, Chen CC, et al. Plasma insulin-like growth factor-binding protein-2 levels as diagnostic and prognostic biomarker of colorectal cancer. J Clin Endocrinol Metab. 2010; 95:1717–25. [PubMed: 20157191]

17. Chen R, Pan S, Yi EC, Donohoe S, Bronner MP, Potter JD, et al. Quantitative proteomic profiling of pancreatic cancer juice. Proteomics. 2006; 6:3871–9. [PubMed: 16739137]

18. Chen R, Brentnall TA, Pan S, Cooke K, Moyes KW, Lane Z, et al. Quantitative proteomics analysis reveals that proteins differentially expressed in chronic pancreatitis are also frequently involved in pancreatic cancer. Mol Cell Proteomics. 2007; 6:1331–42. [PubMed: 17496331]

19. Holmes KM, Annala M, Chua CY, Dunlap SM, Liu Y, Hugen N, et al. Insulin-like growth factor-binding protein 2-driven glioma progression is prevented by blocking a clinically significant integrin, integrin-linked kinase, and NF-kappaB network. Proc Natl Acad of Sci U S A. 2012; 109:3475–80. [PubMed: 22345562]

20. Fujioka S, Sclabas GM, Schmidt C, Frederick WA, Dong QG, Abbruzzese JL, et al. Function of nuclear factor kappaB in pancreatic cancer metastasis. Clin Cancer Res. 2003; 9:346–54. [PubMed: 12538487]

21. Min C, Eddy SF, Sherr DH, Sonenshein GE. NF-kappaB and epithelial to mesenchymal transition of cancer. J Cell Biochem. 2008; 104:733–44. [PubMed: 18253935]

22. Maier HJ, Schmidt-Strassburger U, Huber MA, Wiedemann EM, Beug H, Wirth T. NF-kappaB promotes epithelial-mesenchymal transition, migration and invasion of pancreatic carcinoma cells. Cancer Lett. 2010; 295:214–28. [PubMed: 20350779]

23. Huber MA, Azoitei N, Baumann B, Grunert S, Sommer A, Pehamberger H, et al. NF-kappaB is essential for epithelial-mesenchymal transition and metastasis in a model of breast cancer progression. J Clin Invest. 2004; 114:569–81. [PubMed: 15314694]

24. Chua HL, Bhat-Nakshatri P, Clare SE, Morimiya A, Badve S, Nakshatri H. NF-kappaB represses E-cadherin expression and enhances epithelial to mesenchymal transition of mammary epithelial

cells: potential involvement of ZEB-1 and ZEB-2. Oncogene. 2007; 26:711–24. [PubMed: 16862183]

25. Sun Y, Yokoi K, Li H, Gao J, Hu L, Liu B, et al. NGAL expression is elevated in both colorectal adenoma-carcinoma sequence and cancer progression and enhances tumorigenesis in xenograft mouse models. Clin Cancer Res. 2011; 17:4331–40. [PubMed: 21622717]
26. Kang Y, Zhang R, Suzuki R, Li SQ, Roife D, Truty MJ, et al. Two-dimensional culture of human pancreatic adenocarcinoma cells results in an irreversible transition from epithelial to mesenchymal phenotype. Lab Invest. 2015; 95:207–22. [PubMed: 25485535]
27. Zhao T, Ren H, Li J, Chen J, Zhang H, Xin W, et al. LASP1 is a HIF1alpha target gene critical for metastasis of pancreatic cancer. Cancer Res. 2015; 75:111–9. [PubMed: 25385028]
28. Yang D, Sun Y, Hu L, Zheng H, Ji P, Pecot CV, et al. Integrated analyses identify a master microRNA regulatory network for the mesenchymal subtype in serous ovarian cancer. Cancer Cell. 2013; 23:186–99. [PubMed: 23410973]
29. Carneiro FR, Ramalho-Oliveira R, Mognol GP, Viola JP. Interferon regulatory factor 2 binding protein 2 is a new NFAT1 partner and represses its transcriptional activity. Mol Cell Biol. 2011; 31:2889–901. [PubMed: 21576369]
30. Arsura M, Mercurio F, Oliver AL, Thorgeirsson SS, Sonenshein GE. Role of the IkappaB kinase complex in oncogenic Ras- and Raf-mediated transformation of rat liver epithelial cells. Mol Cell Biol. 2000; 20:5381–91. [PubMed: 10891479]
31. Dunlap SM, Celestino J, Wang H, Jiang R, Holland EC, Fuller GN, et al. Insulin-like growth factor binding protein 2 promotes glioma development and progression. Proc Natl Acad of Sci U S A. 2007; 104:11736–41. [PubMed: 17606927]
32. Asano T, Yao Y, Zhu J, Li D, Abbruzzese JL, Reddy SA. The PI 3-kinase/Akt signaling pathway is activated due to aberrant Pten expression and targets transcription factors NF-kappaB and c-Myc in pancreatic cancer cells. Oncogene. 2004; 23:8571–80. [PubMed: 15467756]
33. Liou HC, Baltimore D. Regulation of the NF-kappa B/rel transcription factor and I kappa B inhibitor system. Curr Opin Cell Biol. 1993; 5:477–87. [PubMed: 8352966]
34. Sierzega M, Popiela T, Kulig J, Nowak K. The ratio of metastatic/resected lymph nodes is an independent prognostic factor in patients with node-positive pancreatic head cancer. Pancreas. 2006; 33:240–5. [PubMed: 17003644]
35. Maier HJ, Wirth T, Beug H. Epithelial-mesenchymal transition in pancreatic carcinoma. Cancers. 2010; 2:2058–83. [PubMed: 24281218]
36. Lamouille S, Xu J, Derynck R. Molecular mechanisms of epithelial-mesenchymal transition. Nat Rev Mol Cell Biol. 2014; 15:178–96. [PubMed: 24556840]
37. Grau AM, Zhang L, Wang W, Ruan S, Evans DB, Abbruzzese JL, et al. Induction of p21waf1 expression and growth inhibition by transforming growth factor beta involve the tumor suppressor gene DPC4 in human pancreatic adenocarcinoma cells. Cancer Res. 1997; 57:3929–34. [PubMed: 9307274]
38. Truty MJ, Urrutia R. Basics of TGF-beta and pancreatic cancer. Pancreatology. 2007; 7:423–35. [PubMed: 17898532]
39. Liu F, Korc M. Cdk4/6 inhibition induces epithelial-mesenchymal transition and enhances invasiveness in pancreatic cancer cells. Mol Cancer The. 2012; 11:2138–48.
40. Rengifo-Cam W, Umar S, Sarkar S, Singh P. Antiapoptotic effects of progastrin on pancreatic cancer cells are mediated by sustained activation of nuclear factor-{kappa}B. Cancer Res. 2007; 67:7266–74. [PubMed: 17671195]
41. Wu Y, Deng J, Rychahou PG, Qiu S, Evers BM, Zhou BP. Stabilization of snail by NF-kappaB is required for inflammation-induced cell migration and invasion. Cancer Cell. 2009; 15:416–28. [PubMed: 19411070]
42. Sun Y, Hu L, Zheng H, Bagnoli M, Guo Y, Rupaimoole R, et al. MiR-506 inhibits multiple targets in the epithelial-to-mesenchymal transition network and is associated with good prognosis in epithelial ovarian cancer. J Pathol. 2015; 235:25–36. [PubMed: 25230372]
43. Wu Y, Diab I, Zhang X, Izmailova ES, Zehner ZE. Stat3 enhances vimentin gene expression by binding to the antisilencer element and interacting with the repressor protein, ZBP-89. Oncogene. 2004; 23:168–78. [PubMed: 14712222]

44. Stanger BZ, Stiles B, Lauwers GY, Bardeesy N, Mendoza M, Wang Y, et al. Pten constrains centroacinar cell expansion and malignant transformation in the pancreas. Cancer Cell. 2005; 8:185–95. [PubMed: 16169464]

45. Chow JY, Ban M, Wu HL, Nguyen F, Huang M, Chung H, et al. TGF-beta downregulates PTEN via activation of NF-kappaB in pancreatic cancer cells. Am J Physiol Gastrointest Liver Physiol. 2010; 298:G275–82. [PubMed: 19940030]

46. Altomare DA, Tanno S, De Rienzo A, Klein-Szanto AJ, Tanno S, Skele KL, et al. Frequent activation of AKT2 kinase in human pancreatic carcinomas. J Cell Biochem. 2002; 87:470–6. [PubMed: 14735903]

47. Mehrian-Shai R, Chen CD, Shi T, Horvath S, Nelson SF, Reichardt JK, et al. Insulin growth factor-binding protein 2 is a candidate biomarker for PTEN status and PI3K/Akt pathway activation in glioblastoma and prostate cancer. Proc Natl Acad of Sci U S A. 2007; 104:5563–8. [PubMed: 17372210]

48. Shen X, Xi G, Maile LA, Wai C, Rosen CJ, Clemmons DR. Insulin-like growth factor (IGF) binding protein 2 functions coordinately with receptor protein tyrosine phosphatase beta and the IGF-I receptor to regulate IGF-I-stimulated signaling. Mol Cell Biol. 2012; 32:4116–30. [PubMed: 22869525]

49. Xi G, Wai C, DeMambro V, Rosen CJ, Clemmons DR. IGFBP-2 directly stimulates osteoblast differentiation. J Bone Miner Res. 2014; 29:2427–38. [PubMed: 24839202]

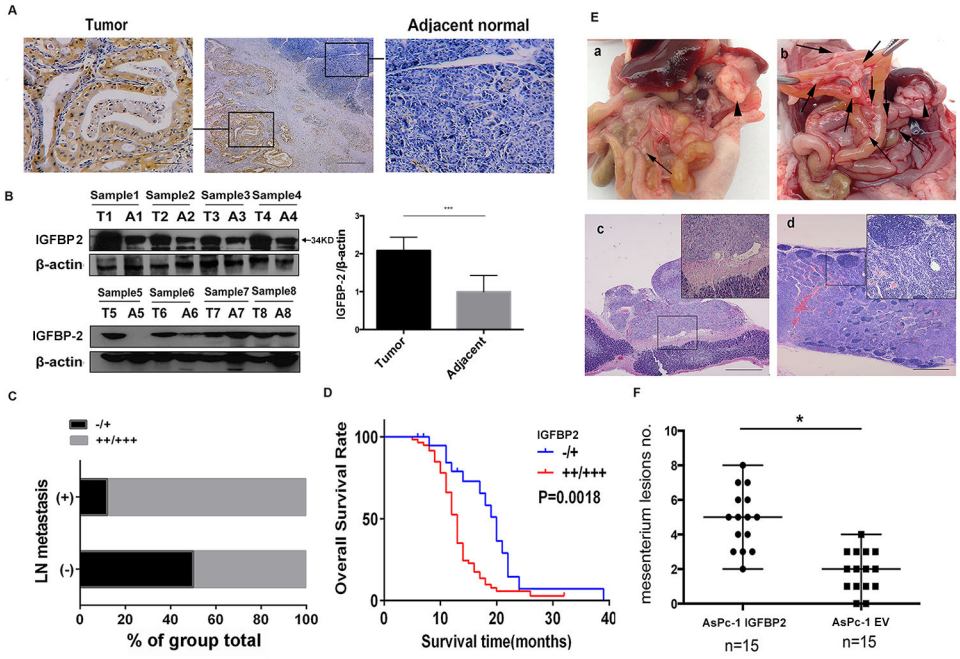

Figure 1. IGFBP2 overexpression in PDAC correlates with lymph node metastasis and shorter survival

(A) IGFBP2 expression in representative PDACs and adjacent normal pancreatic tissues (magnification: middle subpanel 40×, side subpanels 200×). (B) Left panel: western blotting of proteins extracted from eight paired samples of tumor (T) and adjacent normal (A) tissue. Right panel: densitometric quantification of blot results (***P<0.001). (C) Distribution of IGFBP2 expression intensity in lymph node (LN) metastasis or non-metastasis subgroups. (D) Association between tumor IGFBP2 expression levels and overall survival in 80 PDAC patients (P=0.0018 by log-rank test). (E) Orthotopic xenograft pancreatic cancer mouse models generated by injecting AsPc-1 cells transfected with empty vector (EV; subpanel a) or IGFBP2-expressing AsPc-1 cells (subpanel b). Hematoxylin and eosin staining verified mesenteric lesions (subpanel c) and metastatic lymph nodes (subpanel d). Arrowheads indicate primary pancreatic tumor and arrows indicate mesenteric metastatic lesions. (F) Statistical analysis of the total number of visible metastatic lesions in the mesentery. Data are presented as means±SD; *P<0.05.

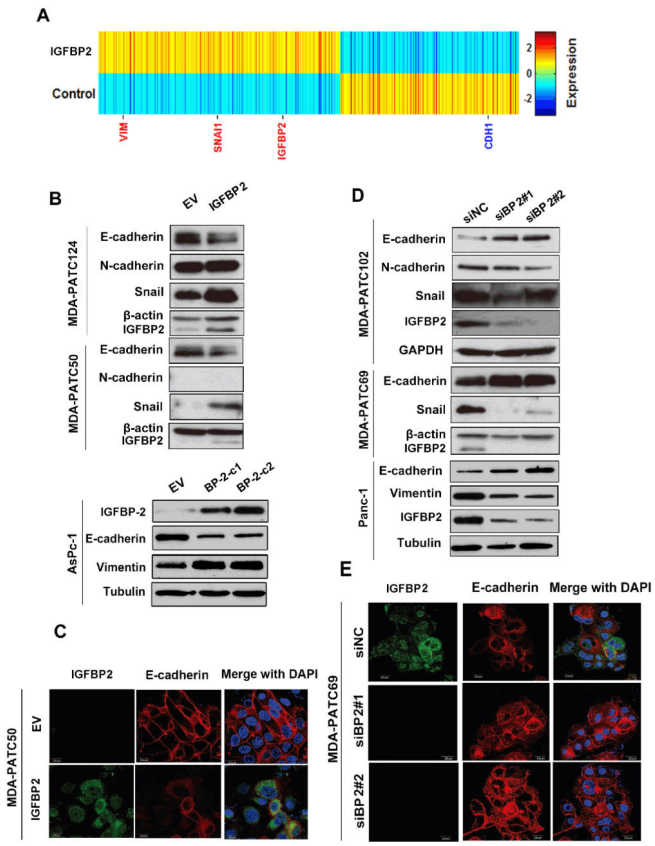

Figure 2. IGFBP2 induces EMT in PDAC cells

(A) The heatmap was generated from mRNA microarray analysis of total RNA extracted from IGFBP2-overexpressing AsPc-1 mixed populations and controls (transfected with empty vector [EV]). (B) Western blot of proteins extracted from two different AsPc-1 IGFBP2-expressing stable clones (C1: Clone,1 C2: Clone2) and PDX cell lines MDA-PATC124 and MDA-PATC50 transiently transfected with EV or IGFBP2 expression plasmids. (C) Confocal images of representative IGFBP2-overexpressing MDA-PATC50 cells stained for IGFBP2 (green) and E-cadherin (red). (D) Western blot of protein extracted from PANC-1 cells and PDX cell lines MDA-PATC102 and MDA-PATC69 transfected with control siRNA (siNC) or one of two IGFBP2 siRNAs (siBP2#1 and siBP2#2). (E) Confocal images of representative IGFBP2-knockdown MDA-PATC69 cells stained for IGFBP2 (green) and E-cadherin (red). In confocal images, cell nuclei were stained with DAPI (blue). Scale bars: 20 μm.

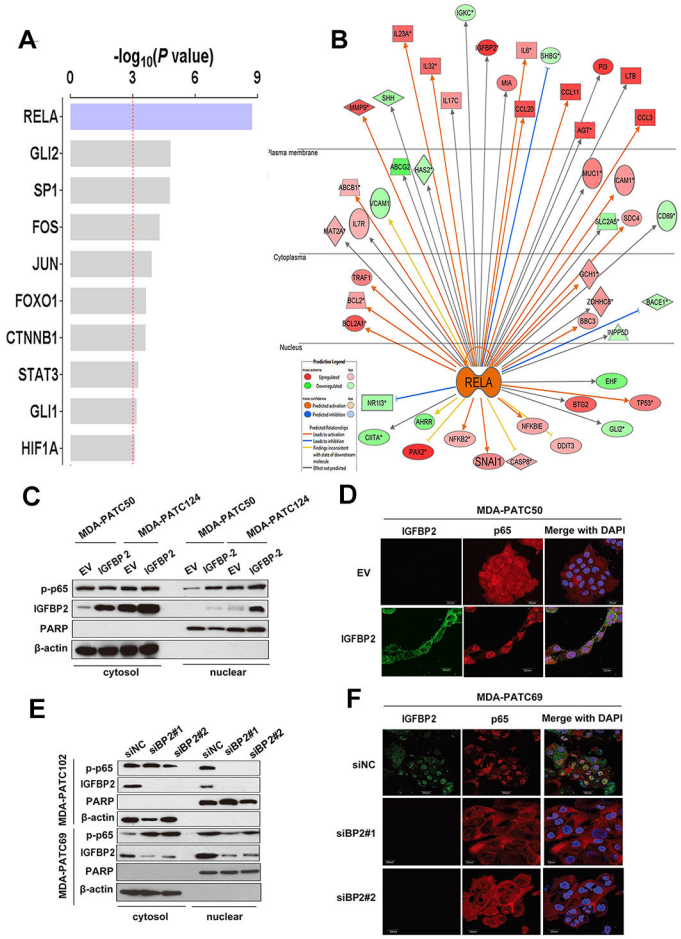

Figure 3. NF-κB is activated and involved in IGFBP2 induction of EMT

(A) The -log overlap *P*-values of the top transcriptional factors enriched from upregulated genes in IGFBP2-overexpressing AsPc-1 cells were identified by Ingenuity Pathway Analysis (IPA). (B) Gene network showing the connections between RELA (p65) and genes downstream of NF-κB was generated by IPA. Red molecules in the network represent the genes that were upregulated upon IGFBP2 overexpression in AsPc-1 cells. Green molecules represent the downregulated genes. (C) Western blot of fractionated MDA-PATC50 and MDA-PATC124 cells transiently transfected with empty vector (EV) or IGFBP2 expression plasmid for 72 hours. (D) Confocal images of IGFBP2 (green) and p65 (red) in representative IGFBP2-overexpressing MDA-PATC50 cells. (E) Western blot of fractionated MDA-PATC102 and MDA-PATC69 cells transiently transfected with siRNA negative control (siNC) or one of two different IGFBP2 siRNAs (siBP2#1 and siBP2#2) for 72 hours to knock down IGFBP2. (F) Confocal images of IGFBP2 (green) and p65 (red) in representative IGFBP2-knockdown MDA-PATC69 cells. In confocal images, cell nuclei were stained with DAPI (blue). Scale bars: 20 μm.

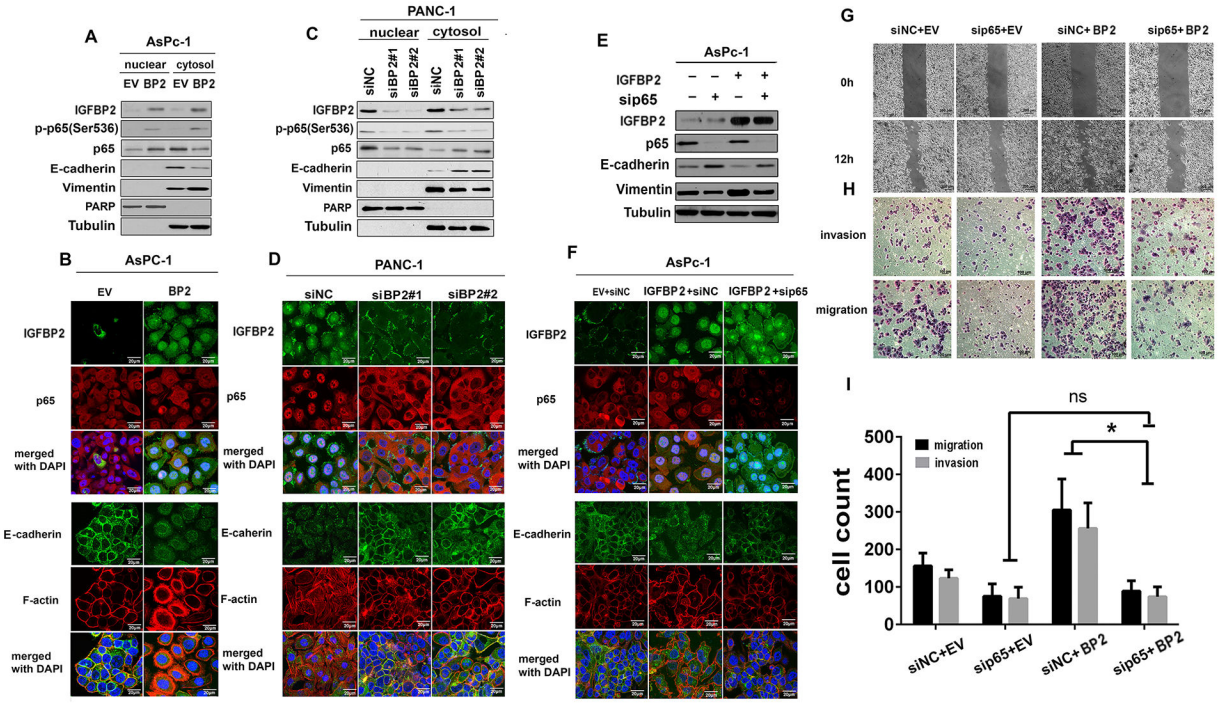

Figure 4. IGFBP2 promotes EMT through NF-κB signaling

(A) Western blot of fractionated AsPc-1 cells transiently transfected with empty vector (EV) or IGFBP2 expression plasmid for 72 hours. (B) Confocal images of IGFBP2 (upper, green), p65 (upper, red), E-cadherin (lower, green), and F-actin (lower, red) in representative stable IGFBP2-overexpressing AsPc-1 cells. (C) and (D) The same experiments as in (A) and (B) were performed in PANC-1 cells transfected with siRNA negative control (siNC) or one of two different IGFBP2 siRNAs (siBP2#1 and siBP2#2) for 72 hours to knock down IGFBP2. (E) AsPc-1 cells were transfected with sip65, IGFBP2 plasmid alone (IGFBP2), or the combination of sip65 and IGFBP2 plasmid. Seventy-two hours after transfection, whole-cell lysates were subjected to western blot. (-) represents cells transfected with either negative control siRNA or EV plasmid. (F) Confocal images of IGFBP2 (upper, green), p65 (upper, red), E-cadherin (lower, green), and F-actin (lower, red) in representatives of the same cell populations as in (E). In confocal images, cell nuclei were stained with DAPI (blue). Scale bars: 20 μm. (G) AsPc-1 cells were transfected with sip65 alone or with the IGFBP2 plasmid (IGFBP2). Seventy-two hours after transfection, the motility of the cells was evaluated by the wound healing assay. (H) Migration and invasive properties of the same cells described in (G) were determined by transwell migration/invasion assays. (I) Quantification of migration and invasion assay data (each experiment performed in triplicate); ns, not significant; *P<0.05.

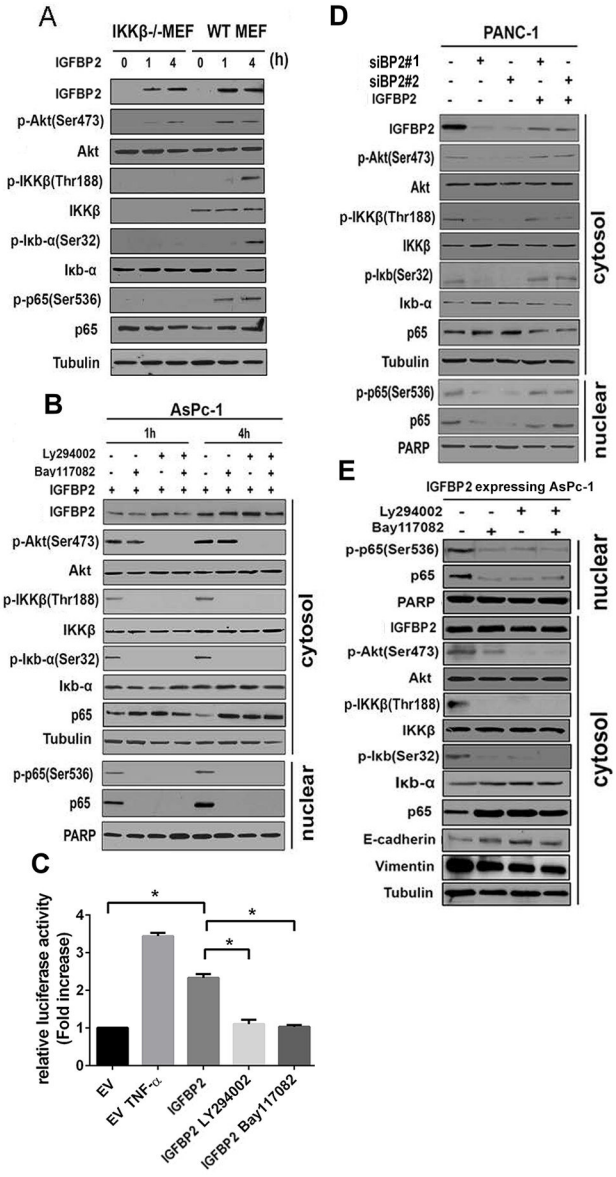

Figure 5. IGFBP2 mediates regulation of NF-κB via the Akt/IKKβ/p65 pathway during EMT

(A) Serum-starved IKKβ knockout mouse embryo fibroblasts (IKKβ$^{-/-}$ MEF) and wild-type MEFs (WT MEF) were stimulated with IGFBP2 recombinant protein (100 ng/mL) for the indicated periods. Whole-cell lysates were subjected to western blot. (B) Serum-starved AsPc-1 cells were pretreated with PI3K inhibitor Ly294002 (50 μM) or IKK inhibitor Bay117082 (20 μM) for 1 hour, followed by stimulation with IGFBP2 recombinant protein (100 ng/mL) for the indicated periods. Fractionated cell lysates were then subjected to western blot. (C) AsPc-1 cells were co-transfected with pGL4.32 (luc2NF-κB-RE/Hygro) vector and pRL4-TK *Renilla* luciferase constructs. After 24 hours, the cells were further transfected with empty vector (EV) or IGFBP2 expression plasmid. Some of the IGFBP2-transfected cells were pretreated with Ly294002 (50 μM) or Bay117082 (20 μM) for 1 hour. The dual luciferase reporter assay was performed 24 hours after transfection of IGFBP2.

Each assay was performed in triplicate and all firefly luciferase values were normalized to *Renilla* luciferase readings (**P*<0.05). EV-transfected cells treated with TNF-α (50 ng/mL) for 1 hour after transfection were used as a positive control. (D) PANC-1 cells were transfected with one of two different IGFBP2 siRNAs (siBP2#1 or siBP2#2) to knock down IGFBP2. Seventy-two hours after transfection, the cells were stimulated with IGFBP2 recombinant protein (100 ng/mL) for 4 hours, and then fractionated cell lysates were subjected to western blot. (E) Stable IGFBP2-overexpressing AsPc-1 cells were treated with Ly294002 (50 μM) or Bay117082 (20 μM) for 4 hours and fractionated cell lysates were subjected to western blot.

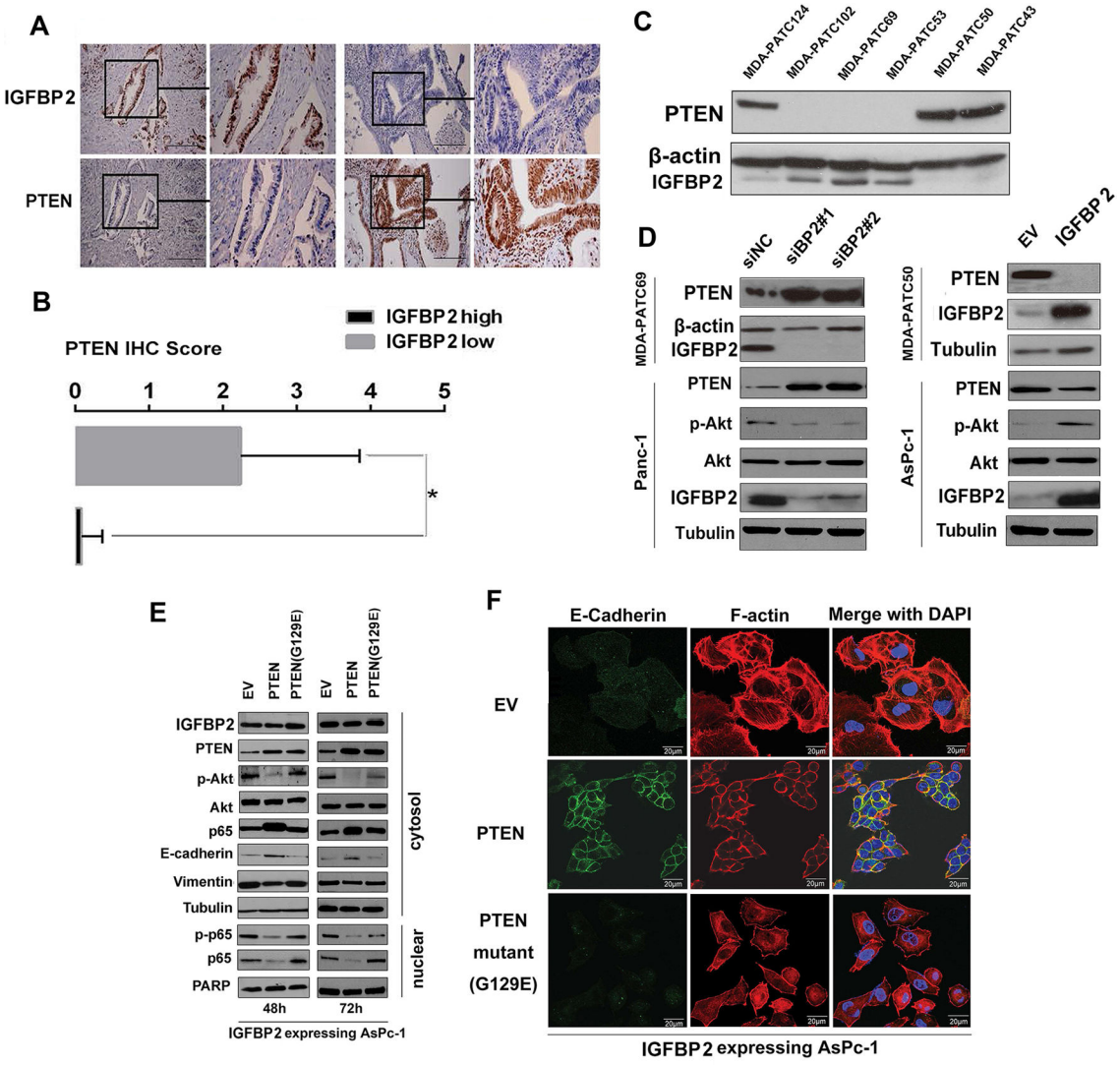

Figure 6. IGFBP2 suppresses PTEN to facilitate Akt activation and p65 nuclear translocation during EMT

(A) IHC staining of IGFBP2 and PTEN in representative tumors from high- and low-IGFBP2–expressing patient groups (magnification: 200× and 400×). (B) Bar charts show the association between IGFBP2 expression and PTEN expression. Error bars represent ± SD. **P*<0.01. (C) Cell lysates from PDX cell lines were subjected to western blot. (D) MDA-PATC69 and PANC-1 cells were transfected with control siRNA (siNC) or one of two different IGFBP2 siRNAs (siBP2#1 or siBP2#2), while MDA-PATC50 and AsPc-1 cells were transfected with empty vector (EV) or IGFBP2 expression plasmid for 72 hours. Cell lysates were then subjected to western blot. (E) Stable IGFBP2-expressing AsPc-1 cells were transfected with EV, wild-type PTEN, or G129E-mutant PTEN plasmids. At 48 hours and 72 hours after transfection, cells were fractionated and cell lysates were subjected to western blot. (F) Confocal images of E-cadherin (green) and F-actin (red) in representatives of the same cell populations as in (D). Cell nuclei were stained with DAPI (blue). Scale bars: 20 μm.

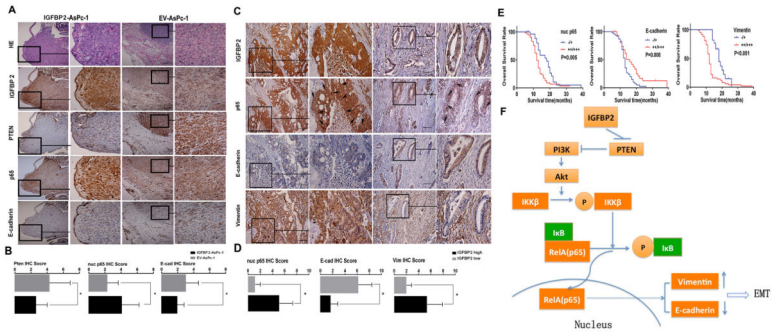

Figure 7. Expression of IGFBP2, PTEN, p65, and EMT markers in PDAC specimens is associated with lymph node metastasis and patient prognosis

(A) IHC staining of IGFBP2, PTEN, p65, and E-cadherin in consecutive sections of representative tumors from orthotopic PDAC nude mouse models constructed by injecting mice with AsPc-1 cells transfected with IGFBP2 expression plasmids (n=15) or empty vehicle (n=15) (magnification: 200× and 400×). (B) Bar charts show the associations between expression of IGFBP2 and expression of PTEN, nuclear (nuc) p65, or E-cadherin (E-cad). Error bars represent ± SD; **P*<0.05. (C) IHC staining of IGFBP2, p65, E-cadherin, and vimentin in representative PDAC samples from groups of patients whose tumor expressed a high (n=59) or low (n=21) level of IGFBP2. The arrows indicate positive or negative staining of nuclear p65 (magnification: 200× and 400×). (D) Bar charts show the association between IGFBP2 expression and nuclear (nuc) p65, E-cadherin (E-cad), or vimentin (Vim) expression. Error bars represent ± SD; **P*<0.01. (E) Kaplan–Meier overall survival curves in high- and low-expressing nuclear p65, E-cadherin, and vimentin groups. (F) Proposed model of IGFBP2-mediated regulation of the PTEN/Akt/IKKβ/p65 axis during EMT in PDAC cells.